JOURNAL OF MODERN SCIENCE
SPECIAL ISSUE
3/57/2024
www.jomswsge.com

DOI: doi.org/10.13166/jms/191398

Daria Stefańczak
WSEI University in Lublin, Poland
ORCID iD: orcid.org/0009-0003-6297-3473

Marcin Dziadosz
Lublin University of Technology, Poland
ORCID iD: orcid.org/0000-0002-0506-6653

Katarzyna Iskra
WSEI University in Lublin, Poland
ORCID iD: orcid.org/0009-0008-2252-3036

Piotr Bednarczuk
WSEI University in Lublin, Poland
ORCID iD: orcid.org/0000-0003-1933-7183

3D MODELING OF THE URINARY BLADDER USING ELECTRICAL IMPEDANCE TOMOGRAPHY: ADVANCED RECONSTRUCTION ALGORITHMS AND MEDICAL APPLICATIONS

MODELOWANIE 3D PĘCHERZA MOCZOWEGO ZA POMOCĄ TOMOGRAFII IMPEDANCYJNEJ: ZAAWANSOWANE ALGORYTMY REKONSTRUKCJI I ZASTOSOWANIA MEDYCZNE

Abstract

Purpose: The research presented in this paper was conducted to obtain a detailed 3D model of the urinary bladder using electrical impedance tomography, a noninvasive tomographic technique.

Methods: Electrical impedance tomography (EIT) is an imaging technique that measures electrical impedance inside the human body. Many methods, including those based on physical models and machine learning, are used to reconstruct the considered 3D object using EIT. The work focuses on the Gauss-Newton algorithm in its generalized form.

Results: Three-dimensional reconstructions of the urinary bladder were obtained. The models are built with high accuracy and can be processed by subsequent algorithms.

Discussion: The constructed models can serve as the basis for correct diagnosis in medicine and as research material for subsequent work, for example, on the possibilities of 3D printing. Possible methods of obtaining even higher-quality reconstruction also remain to be considered.

Streszczenie

Cel: Badania zaprezentowane w pracy zostały przeprowadzone w celu uzyskania szczegółowego modelu 3D pęcherza moczowego z wykorzystaniem nieinwazyjnej techniki tomograficznej, elektrycznej tomografii impedancyjnej.

Metody: Elektryczna tomografia impedancyjna (EIT) to technika obrazowania wykorzystująca pomiar impedancji elektrycznej wewnątrz ciała człowieka. Istnieje wiele metod rekonstrukcji rozważanego obiektu 3D za pomocą EIT, w tym opartych na modelach fizycznych i uczeniu maszynowym. W pracy skupiono się na algorytmie Gaussa-Newtona w postaci uogólnionej.

Wyniki: Otrzymane zostały rekonstrukcje pęcherza moczowego w wersji trójwymiarowej. Modele są zbudowane z dużą dokładnością i mogą być również przetwarzane przez kolejne algorytmy.

Omówienie: Zbudowane modele mogą służyć za podstawę prawidłowego diagnozowania w medycynie i spełniać rolę materiału badawczego do kolejnych prac, na przykład w kierunku możliwości potencjalnego druku 3D. Do rozważenia pozostają również ewentualne metody uzyskania rekonstrukcji jeszcze wyższej jakości.

Keywords: *urinary bladder, 3D modeling, reconstruction, electrical impedance tomography, tomographic measurements, algorithms*

Słowa kluczowe: *pęcherz moczowy, modelowanie 3D, rekonstrukcja, elektryczna tomografia impedancyjna, pomiary tomograficzne, algorytmy*

Introduction

3D modeling is the digital representation of any object or surface (Chen, 2024; Hegazy et al., 2024; Kudashkina et al., 2024). In the most basic case, a three-dimensional model can be created from simple shapes such as cubes, rectangles, and triangles. These shapes are then modified into complex, polygonal designs. The most important terms in the context of 3D modeling are as follows:

- Vertex, a single point and smallest element of a 3D model.
- Edge, a straight line connecting two vertices that helps determine the shape of the 3D model.

Polygon: any shape created by connecting straight lines. Depending on the number of sides and the size of the angles, there are several types of polygons (equilateral, rectangular, regular, irregular, cyclic, convex, and concave).

The face is the most basic part of the polygon mesh. It helps fill the space between the edges. When flat surfaces in the model are *covered,* they create the so-called face.

- Mesh, a set of polygons connected to their surfaces, edges, and vertices. A 3D object consists of one or more meshes.

3D modeling has a wide range of applications. It facilitates the transfer of ideas and is used to create interactive designs of objects or surfaces that represent the actual design. It is also possible to check the structural feasibility of the project. For example, part of a physical object can be created quickly, then the physical properties can be analyzed and the model updated as needed. Unsurprisingly, 3D modeling can be both time – and cost-effective. The 3D model of the urinary bladder is an essential medical tool (Sokolov et al., 2024). 3D models allow doctors and surgeons to plan medical procedures precisely. Before surgery, you can see what the bladder looks like in three-dimensional space, which makes it easier to choose appropriate techniques and tools. 3D objects help in understanding the anatomical relationships between organs. Doctors can better assess how changes in the bladder affect other structures in the area. 3D projects enable the simulation of various scenarios, such as tumor removal or implant placement. Doctors can practice on models before performing actual surgery. A breakthrough was obtaining a urinary bladder using 3D printing. In the United States, a team of scientists implanted an enlarged bladder in a patient, opening up new possibilities in the field of regenerative medicine (Anwar et al., 2023; Beetz et al., 2024; Kudashkina et al., 2024).

Research Methodology

Electrical impedance tomography is an imaging method that measures electrical impedance inside the tested object (Dziadosz et al., 2024; Kozłowski et al., 2020). In EIT, the Gauss-Newton algorithm in the generalized form is very often used for reconstruction problems (Przysucha et al., 2023; Rymarczyk and Tchorzewski, 2018). The reconstruction of the image of the interior of the examined object is related to the determination of the minimum of the objective function, which in the considered case is defined as follows:

$$F(\sigma) = \frac{1}{2}\left(\| U(\sigma) - U_m \|^2 + \lambda^2 \| R^T R \{ \sigma - \sigma^* \} \|^2 \right),$$

where:

σ – proper conductivity,

σ^* – specific conductivity assumed a priori – represents the known properties of the object's interior,

$U(\sigma)$ – voltages obtained via numerical calculations (FEM),

U_m – voltages obtained as a result of measurements carried out using a tomograph,

R – regularization matrix, usually it is an identity matrix (with Tikhonov regularization (Rymarczyk et al., 2024)) or a discrete approximation of the selected differential operator (with Laplace regularization) in the form of a diagonal matrix raised to a specific power (with power-law regularization),

λ – regularization parameter – positive actual number.

Using appropriate approximations, it can be shown that the following formula gives the specific conductivity in the iteration number k + 1:

$$\sigma_{k+1} = \sigma_k - \alpha_k \left(S_k^T S_k + \lambda^2 R^T R \right)^{-1} \left[S_k^T \{ U(\sigma_k) - U_m \} + \lambda^2 R^T R \{ \sigma_k - \sigma^* \} \right],$$

where:

$$S_k = \left[\frac{\partial U(\sigma)}{\partial \sigma} \right]_{\sigma=\sigma_k},$$

and:

S_k – sensitivity matrix calculated in the k-th step,
α_k – k-th step length factor [step length],
σ^* – a priori solution (we consider the second backward $\sigma^* = \sigma_{k-1}$, $k > 1$).

The step length factor was determined as follows:

1. Let $0 < \alpha_{init} \leq 1$, $l = 0$, $\alpha_0 = \alpha_{init}$.
2. Until $f(\sigma_k + \alpha_k p_k) > f(\sigma_k)$
   a. $\alpha_k *= \frac{\tau}{l+1}$, for e.g. $\tau = \frac{1}{2}$, $\tau \in (0,1)$,
   b. $l += 1$,

where $p_k = -(S_k^T S_k + \lambda^2 R^T R)^{-1} [S_k^T \{U(\sigma_k) - U_m\} + \lambda^2 R^T R \{\sigma_k - \sigma^*\}]$ and $f(x)$ is the objective function.

The Gauss-Newton algorithm is used in image reconstruction to reverse the degradation process and recreate the original image from the degraded version (Liu et al., 2024; Mahale and Singh, 2024; Pillutla et al., 2023). Before performing reconstruction, it is important to determine how the image was degraded. The degradation process may include interference during image capture or transmission, lighting effects on the image sensor, and various types of noise. The Gauss-Newton algorithm is based on a mathematical model that combines the original image (f(x,y)) with the observed image (g(x,y)). This model takes into account the image degradation function (h(x,y)) and noise characteristics (n(x,y)):

$$g(x,y) = f(x,y) * h(x,y) + n(x,y).$$

(h(x,y)) represents a degradation function that can be known or estimated, while (n(x,y)) is noise that can have various distributions such as Gaussian, uniform, or Poisson. The Gauss-Newton algorithm works iteratively (Loke and Dahlin, 2002; Morrison, 2013; Siregar et al., 2018). In each iteration, new approximations of the degradation model parameters are calculated, minimizing the sum of the squares of the differences between the observed and reconstructed images. Various filtering techniques are used to reconstruct the image. Averaging filters, median filters, and other methods help reduce visible noise and improve the quality of the reproduced image. In the case of filters and degradation models, it is important to select the appropriate parameters. Incorrect selection may affect the whole process. Image reconstruction using the Gauss-Newton algorithm is used in fields such as medicine, image processing, materials analysis, and scientific research (Gholami, 2024; Hanif, 2024; Yudin, 2021).

Laplace regularization matrix

In the case of tetrahedra, for each tetrahedron i, we determine its neighbors (the set of indexes of elements neighboring to i – th):

$$L_{ij} = \begin{cases} \overline{\overline{N_\iota}}, & dla\ \ j = i \\ -1 & dla\ j \in N_i. \\ 0\ in\ other\ cases \end{cases}$$

The neighbor of element i is element j, which has a familiar face with element i. For cubes, there are two forms of the Laplacian (Lebedeva and Ryabov, 2022; Maréchal et al., 2023). The first assumes six direct neighbors for one cube. An element that has a familiar face with the considered element is considered a neighbor. The second assumes that a neighbor is every element that contains at least one node in common with the element under consideration. Table 1 compares exemplary simulations and reconstructions after five iterations of the discussed algorithm.

Table 1. *Comparison of exemplary simulation and reconstruction after five iterations*

Simulation	Reconstruction after five iterations	Objective function
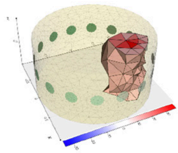	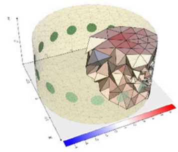	c = 0.0186
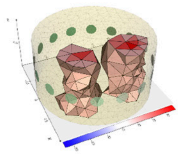	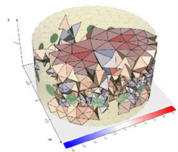	c = 0.0330
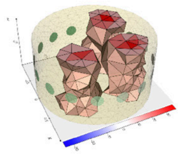	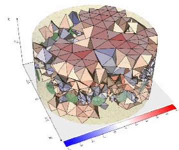	c = 0.0920
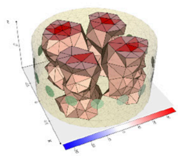	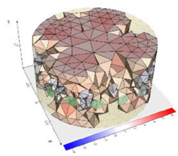	c = 0.0656

Three-dimensional model of the urinary bladder

We model the urinary bladder as a rotational ellipse with the following equation:

$$\frac{x^2}{40^2} + \frac{(y-50)^2}{30^2} + \frac{z^2}{30^2} \leq 1.$$

Figure 1 presents the reconstruction using the Laplace matrix with the Gauss-Newton algorithm for the regularization parameter $\lambda = 0,00001$.

Figure 1. *Urinary bladder reconstruction for dense mesh*

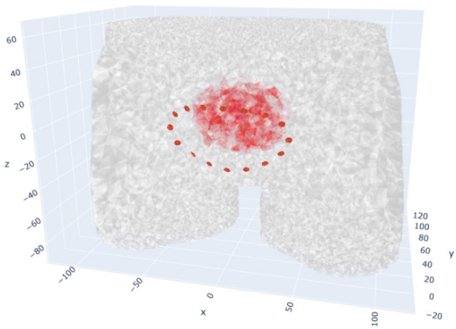

Conclusions

The paper presented the development of a detailed 3D model of the urinary bladder using electrical impedance tomography. The research included the application of the Gauss-Newton algorithm in generalized form, the Laplace regularization matrix, and a three-dimensional model of the urinary bladder (a urinary bladder reconstruction for dense mesh).

3D models of the bladder are essential not only for education and research but also for opening the door to innovative solutions in medicine. Plans include research on improving the quality of the obtained urinary bladder reconstructions. A big challenge is the development of machine learning algorithms that will be used to classify bladder diseases. Such a solution would be non-invasive, significantly improving the patient's diagnosis process. Additionally, such a procedure would be performed much faster and less painful for the examined person, which is often essential.

References

Anwar, S., Bunker, M., Henry, T., Kouretas, P., Harris, I., Agarwal, A. (2023). 3D Modeling in Congenital Cardiac Interventions. 367–375. https://doi.org/10.1007/978-3-030-85408-9_32

Beetz, M., Banerjee, A., Grau, V. (2024). Modeling 3D Cardiac Contraction and Relaxation With Point Cloud Deformation Networks. *IEEE Journal of Biomedical and Health Informatics* PP, 1–10. https://doi.org/10.1109/JBHI.2024.3389871

Chen, Y. (2024). Research on prosthesis customization with 3D modeling and printing technology. *Theoretical and Natural Science* 29, 158–163. https://doi.org/10.54254/2753-8818/29/20240768

Dziadosz, M., Mazurek, M., Stefaniak, B., Wójcik, D., Gauda, K. (2024). A comparative study of selected machine learning algorithms for electrical impedance tomography. *ELECTROTECHNICAL REVIEW* 1(4), 239–242. https://doi.org/10.15199/48.2024.04.47

Gholami, A. (2024). An extended Gauss-Newton method for full waveform inversion. *GEOPHYSICS* 89, 1–55. https://doi.org/10.1190/geo2022-0673.1

Hanif, D. (2024). Gauss-Newton Method for Feedforward Artificial Neural Networks.

Hegazy, M., Cho, Myung, Cho, Min, Lee, S. (2024). 3D Digital Modeling of Dental Casts from Their 3D CT Images with Scatter and Beam-Hardening Correction. *Sensors* 24. https://doi.org/10.3390/s24061995

Kozłowski, E., Rymarczyk, T., Kłosowski, G., Cieplak, T. (2020). Logistic regression in image reconstruction in electrical impedance tomography. *Przeglad Elektrotechniczny* 5, 95–98.

Kudashkina, A., Kamyshanskaya, I., Pavelets, K., Rusanov, D., Kalyuzhnyy, S. (2024). 3D-modeling Capabilities in Assessing Resectability of Pancreatic Head Tumors. *Journal of radiology and nuclear medicine* 104, 244–254. https://doi.org/10.20862/0042-4676-2023-104-4-244-254

Lebedeva, A., Ryabov, V. (2022). Method of moments in the problem of inversion of the Laplace transform and its regularization. *Vestnik of Saint Petersburg University. Mathematics. Mechanics. Astronomy* 9, 46–52. https://doi.org/10.21638/spbu01.2022.105

Liu, Q., Wang, S., Wei, Y. (2024). A Gauss–Newton method for mixed least squares-total least squares problems. *Calcolo* 61, 1–27. https://doi.org/10.1007/s10092-024-00568-2

Loke, M., Dahlin, T. (2002). A comparison of the Gauss-Newton and quasi-Newton methods in resistivity imaging inversion. *Journal of Applied Geophysics* 49, 149–162. https://doi.org/10.1016/S0926-9851(01)00106-9

Mahale, P., Singh, A. (2024). Convergence analysis of simplified Gauss–Newton iterative method under a heuristic rule. *Proceedings – Mathematical Sciences* 134. https://doi.org/10.1007/s12044-024-00777-3

Maréchal, P., Triki, F., Simo, W. (2023). Regularization of the inverse Laplace transform by mollification. *Inverse Problems* 40. https://doi.org/10.1088/1361-6420/ad1609

Morrison, N. (2013). Tracking Filter Engineering: The Gauss-Newton and polynomial filters. https://doi.org/10.1049/PBRA023E

Pillutla, K., Roulet, V., Kakade, S., Harchaoui, Z. (2023). Modified Gauss-Newton Algorithms under Noise.

Przysucha, B., Wójcik, D., Rymarczyk, T., Król, K., Kozłowski, E., Gąsior, M. (2023). Analysis of Reconstruction Energy Efficiency in EIT and ECT 3D Tomography Based on Elastic Net. *Energies* 16(3), 1490. https://doi.org/10.3390/en16031490

Rymarczyk, T., Mazurek, M., Hyka, O., Wójcik, D., Dziadosz, M., Kowalski, M. (2024). Poster Abstract: A Wearable for Non-Invasive Monitoring and Diagnosing Functional Disorders of the Lower Urinary Tract, in: Proceedings of the 21st ACM Conference on Embedded Networked Sensor Systems, SenSys '23. Association for Computing Machinery, New York, NY, USA, 510–511. https://doi.org/10.1145/3625687.3628382

Rymarczyk, T., Tchorzewski, P. (2018). Implementation 3D level set method to solve inverse problem in EIT. 159–161. https://doi.org/10.1109/IIPHDW.2018.8388347

Siregar, R., Tulus, T., Ramli, M. (2018). Analysis Local Convergence of Gauss-Newton Method. *IOP Conference Series: Materials Science and Engineering* 300, 012044. https://doi.org/10.1088/1757-899X/300/1/012044

Sokolov, Y., Topilin, O., Airapetyan, M., Sukhodolskaya, O., Vydysh, S. (2024). The clinical use of 3D-modeling in pediatric surgery. *Archives of Pediatrics and Pediatric Surgery* 1, 24–30. https://doi.org/10.31146/2949-4664-apps-2-2-24-30

Yudin, N. (2021). Modified Gauss-Newton method for solving a smooth system of nonlinear equations. *Computer Research and Modeling* 13, 697–723. https://doi.org/10.20537/2076-7633-2021-13-4-697-723